Microchimica Acta (2019) 186:659
https://doi.org/10.1007/s00604-019-3781-2

ORIGINAL PAPER

Electrochemical thrombin aptasensor based on using magnetic nanoparticles and porous carbon prepared by carbonization of a zinc(II)-2-methylimidazole metal-organic framework

Qian Ren[1] · Xianzhen Xu[1] · Guangping Cao[1] · Jianfei Xia[1] · Zonghua Wang[1] · Qingyun Liu[2]

Received: 5 August 2019 / Accepted: 21 August 2019

Abstract

A homogeneous electrochemical aptasensor was obtained by modifying a glassy carbon electrode (GCE) with a porous carbon nanomaterial (Z-1000, about 70 nm, deteced by transmission electron microscopic) that was obtained by carbonization of a zinc(II)-2-methylimidazole metal-organic framework. Z-1000 possesses a large specific surface and outstanding electrochemical properties. A thrombin-binding aptamer (CP) was immobilized on the magnetite nanoparticles MNPs by the condensation reaction and further combined with reporter probe (RP) that is functionalized with electroactive methylene blue (MB). In the presence of thrombin, the CP was specifically recognized with it to form the CP/MNP/Thb complex, and the RP was dissociated from MNPs. The released RP was captured by the modified GCE through π-stacking interaction between nucleobases and carbon nanostructure. The electrical signal generated by MB can be monitored by differential pulse voltammetry (DPV). Under the optimized conditions, the DPV peak current at around −0.28 V (vs. SCE) increases with thrombin concentration. The sensor has a detection limit of 0.8 fM of thrombin and a linear range that extends from 10 fM to 100 nM. It was successfully applied to the analysis of spiked serum. The recoveries are 98.1–99.4% and RSDs are 3.9%–4.0%. Conceivably, this aptasensor scheme can be easily extended to other proteins and gives inspiration to manufacture sensitive aptasensor.

Keywords Zeolitic imidazolate framework · Porous carbon nanostructure · Magnetic nanomaterial · Electrochemical biosensor · Protein detection

Introduction

Various strategies for aptamer-based protein detection have been designed, including fluorescent aptasensors [1–3], electrochemical aptasensors [4], colorimetric aptasensors [5], surface plasmon resonance aptasensors [6] and so on. Among them, the homogeneous electrochemical aptasensors have got significant attention and been applied widely in bioassay due to its simplicity, rapid response, low steric hindrance, high binding efficiency and allowing the configurational freedom of recognition units compared with heterogeneous assay [7–9]. Thus, using homogeneous electrochemical aptasensor to detect analytes is very effective and highly desirable. However, finding a material with good biocompatibility, high conductivity, and high electron mass transfer efficiency is a huge challenge for building an ultra-sensitive homogeneous electrochemical aptasensor.

Qian Ren and Xianzhen Xu contributed equally to this work.

Electronic supplementary material The online version of this article (https://doi.org/10.1007/s00604-019-3781-2) contains supplementary material, which is available to authorized users.

✉ Jianfei Xia
xiajianfei@126.com

[1] College of Chemistry and Chemical Engineering, Shandong Sino-Japanese Center for Collaborative Research of Carbon Nanomaterials, Collaborative Innovation Center for Marine Biomass Fiber Materials and Textiles, Laboratory of Fiber Materials and Modern Textile, the Growing Base for State Key Laboratory, Qingdao University, Qingdao 266071, People's Republic of China

[2] College of Chemistry and Environmental Engineering, Shandong University of Science and Technology, Qingdao, People's Republic of China

Published online: 30 August 2019

Metal-organic frameworks (MOFs), a class of crystalline porous materials with a large surface areas, large pore capacity and adjustable pore size, have received more attentions [10]. It have been applied in many areas, such as gas storage, adsorption, supercapacitors, catalysis, drug delivery, and sensors [11, 12]. However, the low electrical conductivity of MOFs limits its development in the field of electrochemistry, especially electrochemical biosensing [13]. Therefore, it's challenging to improve the electrochemical conductivity of MOFs and make full use of their excellent performance in electrochemical biosensing. Significantly, using MOFs as ideal precursors and templates for the generation of porous carbon materials to improve the conductivity has received particular attention. And it has been demonstrated that the porous carbon nanomaterials derived from MOFs possess attractive features such as high surface areas, large pore sizes and controlled pore structure [14]. They have good performance in hydrogen storage, unprecedented electrochemical properties and excellent electrochemical capacitances [15, 16]. Furthermore, carbon nanostructures can bind probes via π-stacking interactions between the nucleobases and carbon nanostructure [17]. Tan et al. [18] reported a sensing platform based on magnetic porous carbon nanocomposites derived from MOFs for DNA fluorescent detection. Among these MOFs, ZIF-8 is considered to be an excellent candidate with a high carbon content, ordered holes and stable property [19]. It can be directly carbonized without the need for any additional carbon sources to synthesize nanoporous carbon materials, which enables the easy preparation in one-pot [20, 21]. In addition, the ZIF-8 derived nanoporous carbon can show highly graphitized structure when the pyrolysis temperature reached 1000 °C [22]. The synergistic effects of porous structure and graphene phase can promote electron transfer, which improves sensitivity and selectivity of the detection platform.

In this work, a stable, sensitive and specific homogeneous electrochemical aptasensor has been developed to achieve electrochemical detection of thrombin by using the Z-1000 modified glassy carbon electrode (GCE). The Z-1000 is obtained by direct carbonization of ZIF-8 at 1000 °C. The aptasensor is based on the aptamer-protein specific recognition and π-stacking interaction between nucleobases and carbon nanostructure, achieving sensitive thrombin detection. The thrombin is selected as one model protein analyte, which has a significant impact on human health and is related to many diseases as well. The magnetic nanoparticles (MNPs) have been used to build the aptasensor. The MNPs can be employed as probe carriers and separated from homogeneous solution by magnetic separation. It can not only simplify the experimental procedure but also achieve signal transduction and amplification. Hence we expect that the combination of Z-1000 porous carbon nanostructure and the homogeneous strategy can play a significant role for thrombin detection.

Experimental section

Materials and reagents

Zinc nitrate hexahydrate ($Zn(NO_3)_2 \cdot 6H_2O$) and 2-methylimidazole ($C_4H_6N_2$) were purchased from Aladdin Reagent Co. Ltd. (http://www.aladdin-e.com). 1-ethyl-(3–3′-dimethy-laminopropyl) carbodiimide (EDC) and N-hydroxysuccini-mide (NHS) were supplied by Aladdin Reagent Co., Ltd. (http://www.aladdin-e.com). Carboxyl-modified magnetic nanoparticles (MNPs) were obtained from BaseLine ChromTech Research Centre (http://www.qiuhuan.com). Thrombin (Thb), Lysozyme (Lyz) and Bovine Serum Albumin (BSA) were acquired from Sangon Biotechnology Co., Ltd. (https://www.sangon.com). The oligonucleotides were synthesized and purified by Sangon Biotechnology Co., Ltd. (https://www.sangon.com), and the sequences were provided in Table S1. All of the chemicals were analytical grade and used without further purification. All of the aqueous solutions were prepared by ultrapure water obtained from a Milli-Q water purification system (18.2 MΩ·cm, Millipore Corp., Bedford, MA).

Apparatus

Transmission electron microscopic (TEM) images were recorded by a JEM-1200EX transmission electron microscope (JEOL, Japan). The UV-vis absorption spectra were recorded by a UV-2500 UV-vis spectrophotometer (LabTech). Powder X-ray diffraction (PXRD) patterns were recorded by Rigaku Ultima IV diffractometer. The cyclic voltammograms (CVs) and electrochemical impedance spectroscopy (EIS) measurements were obtained by Princeton PARSTAT 4000A (America), and the differential pulse voltammetry (DPV) measurements were carried out on a CHI-660E electrochemical workstation (Shanghai Chenhua Instruments Co., China) at room temperature. A traditional three-electrode cell was used with a Z-1000 modified GCE as the working electrode, a saturated calomel electrode (SCE) as the reference electrode, and a platinum wire as the auxiliary electrode. All the potentials here were referred to SCE.

Preparation of the porous carbon nanomaterial Z-1000

The ZIF-8 was synthesized using a one-pot reaction method according to the published literature [23]. The detail synthesis shows in the Electronic Supporting Material. The Z-1000 was synthesized by carbonization of ZIF-8 under a flow of Ar atmosphere at 1000 °C for 2 h. After the carbonization, the black powder was collected and used without any further treatment.

Preparation of a Z-1000 modified GCE

Firstly, the GCE was carefully polished with 0.3 and 0.05 μm Al_2O_3 powder to obtain a mirror-like plane. Then it was successively rinsed by ethanol and deionized water, and dried in N_2. The dispersion (2 mg mL^{-1}) was formed by dispersing the Z-1000 in deionized water. Then 5 mL of dispersion was dropped on the clean surface of GCE and dried at room temperature for 3 h to fabricate a modified GCE.

Preparation of DNA probe-modified magentic nanoparticles

Firstly, 60 μL of carboxyl-modified MNPs were washed with 300 μL of phosphate buffer (0.01 M, pH = 7.4 containing 100 mM NaCl) three times. After that, MNPs were dispersed into 120 μL phosphate buffer for further use. 500 μL mixture of EDC (0.1 M) and NHS (0.01 M) were dissolved in MNPs dispersions. To activate carboxyl groups of MNPs, the mixture was incubated at room temperature. Subsequently, the activated MNPs were washed with phosphate buffer three times and then dispersed into 120 μL phosphate buffer. Afterward, 300 μL of amino-modified capture probe (CP, 1 μM) was added into the activated MNPs dispersions and reacted at 37 °C for 12 h to obtain CP/MNPs. The resulted CP/MNPs conjugates were magnetically washed with phosphate buffer three times and redispersed into 120 μL phosphate buffer. Hereafter, 300 μL of methylene blue-modified reporter probe (RP, 1 μM) was added into CP/MNPs conjugates solution and reacted at 37 °C for 1 h in the dark to form the RP/CP/MNPs conjugates. Ultimately, the conjugates were washed with phosphate buffer three times and dispersed into 120 μL phosphate buffer for further use.

Calibration features

In order to prepare the electrochemical aptasensor, different concentrations of thrombin was added into the RP/CP/MNPs conjugates and incubated at room temperature for 2 h. After magnetic separation, the modified GCE was immersed into the upernatant and reacted at room temperature for 50 min. Finally, the resulting Z-1000 modified GCE was rinsed by phosphate buffer and then employed as working electrode to perform electrochemical experiments.

Electrochemical measurements

The CVs and EIS measurements were conducted in 5 mM $K_3[Fe(CN)_6]$ aqueous solution containing 0.1 M KCl. CVs were carried out in the potential range of −0.2 to 0.6 V at a scan rate of 100 mV s^{-1}. EIS was conducted with the frequency changed from 0.01 Hz to 100 kHz, together with 5 mV as the amplitude. The DPV measurements were performed in detection phosphate buffer (10 mM, pH 7.4, containing 2 mM H_2O_2 and 0.3 M NaCl) at a scan rate of 100 mV s^{-1} by scanning the potential in the range from 0 to −0.6 V versus SCE reference electrode. The DPV peak current increased at around −0.28 V. All electrochemical experiments were carried out at room temperature.

Results and discussion

Design principle of the electrochemical aptasensor

The principle of the Z-1000-based homogeneous electrochemical aptasensor for sensitive detection of thrombin is depicted in Scheme 1. In our work, the Z-1000 was obtained by direct carbonization of ZIF-8 and it is employed to modify the working electrode. In Scheme 1b, the aptasensor is constructed by RP/CP/MNP complexes, where the CP is designed as the thrombin aptamer. Firstly, the CP is connected with MNPs through the condensation reaction between amino group at 5′ terminus of CP and carboxyl group on MNP. And the CP further combined with RP which is functionalized with electroactive methylene blue (MB) at 5′ terminus. When the thrombin target is present in solution, the CP will specifically anchor to its target to form CP/MNP/Thb conjugates based on aptamer recognition, resulting in the dissociation of RP. After magnetic separation, the conjugates are present in the precipitate while RP is removed to supernatant. Subsequently, the released RP can be adsorbed on the Z-1000 based on π-stacking interaction between nucleobases and carbon nanostructure. As a result, the generated electronic signal by MB could be monitored through differential pulse voltammetry (DPV) measurements.

Choice of materials

There are three key factors in building this biosensing platform, electrical conductivity, specific area of the material, and binding efficiency with DNA probes. Compared with conventional materials, the porous carbon derived from MOFs is considered as a sort of potential materials with high surface areas, large pore sizes and controlled pore structure [14]. Especially, carbon nanostructures can adsorb DNA by π-stacking interactions between the nucleobases and carbon nanostructure. Among various MOFs, ZIF-8 derived porous carbon possesses stable porous structure and excellent electrochemical properties. The Z-1000 (derived from ZIF-8) with these excellent features is beneficial to improve the performance of the thrombin detection assay.

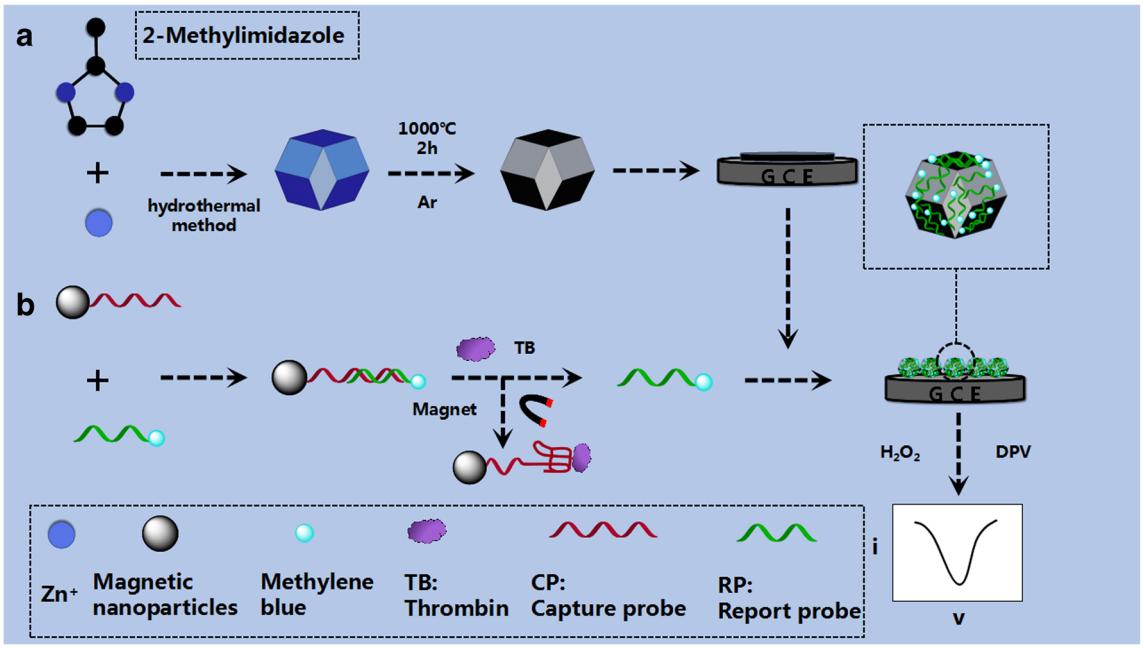

Scheme 1 Schematic illustration of (**a**) the strategy for preparation of the porous carbon nanomaterial Z-1000; and **b** the Z-1000 based homogeneous electrochemical aptasensors for the detection of thrombin

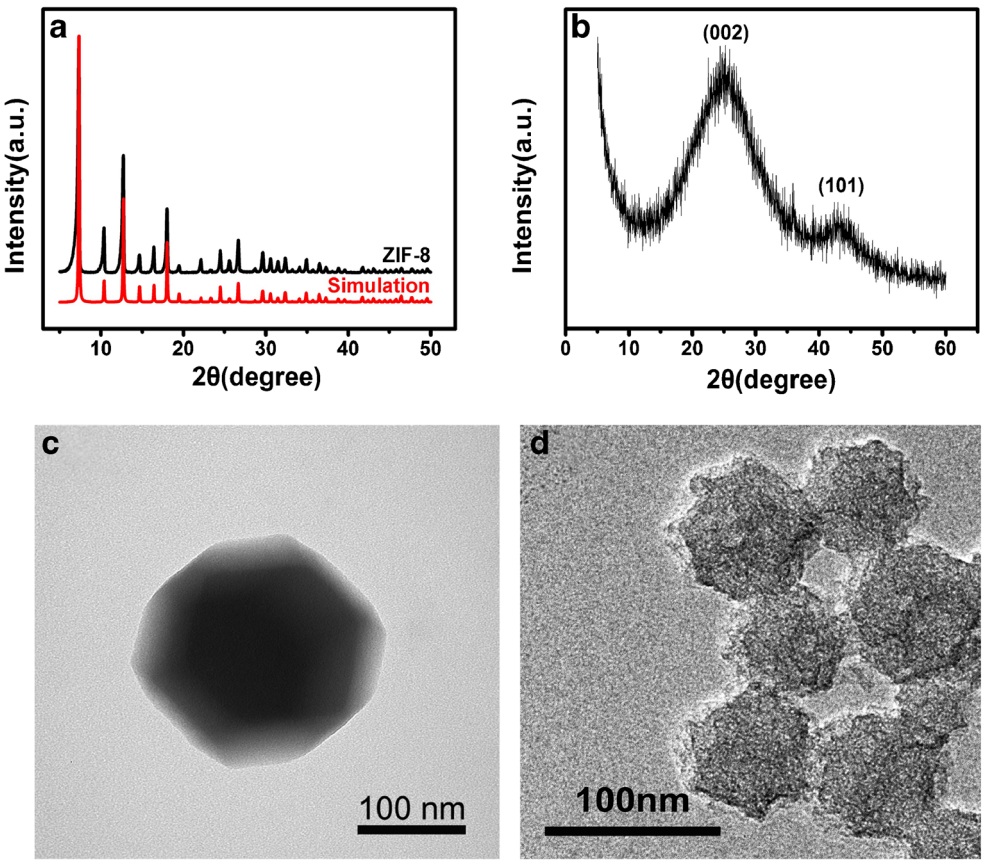

Fig. 1 PXRD patterns of ZIF-8 (**a**) and Z-1000 (**b**) samples. TEM images of ZIF-8 (**c**) and Z-1000 (**d**) samples

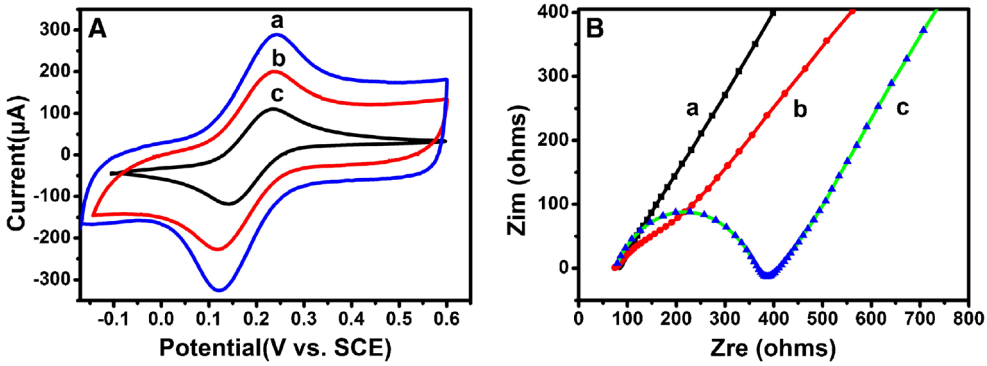

Fig. 2 CVs (**A**) and EIS (**B**) characterization of the porous carbon nanomaterial (Z-1000) modified GCE (a), Z-1000 modified GCE with RP (b) and bare GCE (c) in 5 mM $[Fe(CN)^6]^{3-/4-}$ aqueous solution containing 0.1 M KCl

Characterization of Z-1000 and of Z-1000 modified GCE

The structure and morphological details of ZIF-8 and Z-1000 were characterized by PXRD pattern and TEM image. As shown in Fig. 1a, the PXRD pattern of real ZIF-8 sample has good accordance with simulation curve of ZIF-8, indicating that ZIF-8 has been successfully synthesized. From Fig. 1b, it is noted that the PXRD pattern of Z-1000 displays two broad peaks at 25° and 44° corresponding to carbon (002) and (101) diffractions, respectively. The (002) peaks perform a certain degree of graphitization, meaning that there are parallel single layers in the Z-1000. ZnO is reduced during the carbonization process when the temperature is higher than 800 °C. And when the temperature is higher than 904 °C, the Zn metal (boiling point, 904 °C) will be evaporated. Therefore, there is no peak which related to zinc species in the PXRD data of Z-1000. Figure 1c and d respectively show the TEM images of the ZIF-8 and Z-1000. Figure 1c shows the ZIF-8 has a diameter of about 150 nm. And the ZIF-8 shows the typical rhombic dodecahedron morphology and crystal structure. Compared with ZIF-8, Z-1000 (about 70 nm) shows an apparent irregular margins and bigger holes in carbon materials (Fig. 1d). The reason is that the evaporation of metal nodes and completely of pyrolysis of organic ligands at high temperature. Furthermore, the excellent conductivity of Z-1000 porous carbon is further investigated by CV and EIS plots in Fig. S1. The change of the oxidation peak current and the semicircle diameter of the Nyquist plots can directly reflect the excellent electrochemical performance of the carbon materials. And Fig. S2 is to evaluate the binding stability between Z-1000 and GCE. All these results indicate that the Z-1000 modified GCE electrode demonstrates outstanding electrochemical properties and possesses excellent binding stability at the interface between the Z-1000 and GCE, which would benefit for the construction of electrochemical aptasensors with improved performances.

Electrochemical characterization of the sensor

Figure 2A shows the CV plots of the electrochemical aptasensor. When the thrombin is present, the disassociated RP can be adsorbed on the Z-1000 surface. The oxidation peak current obviously decreases to 199.89 μA (curve b) that is lower than that obtained by Z-1000 modified GCE (290.15 μA, curve a) but still higher than bare GCE (110.06 μA, curve c). The change of redox peak current is ascribed to the adsorption of probes on the surface of porous carbon which leading to obstruction of electron conduction. At the same time, the same results have been presented by the EIS curves (Fig. 2B). When the thrombin target is present in solution, a impedance (curve b) appears, which is slightly higher than the Z-1000 modified GCE (curve a) but much lower than the bare GCE (curve c). Therefore, the probes block electron conduction and increase resistance. In a nutshell, the experimental results state the well adsorption between the reporter probes and Z-1000 modified GCE.

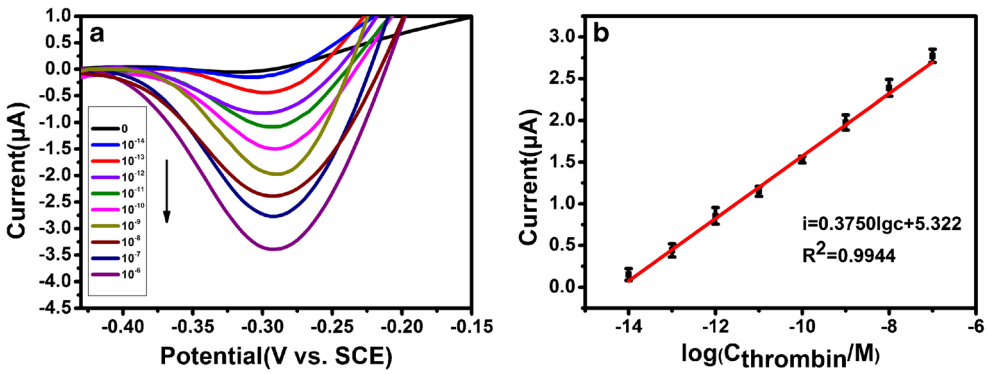

Fig. 3 DPV responses of the homogeneous electrochemical aptasensor based on Z-1000 to different concentrations of thrombin (from 10 fM to 1 μM) at scan rate of 100 mV s^{-1} with working voltage from 0 to −0.6 V (**a**). The calibration plots of peak currents and thrombin concentration (**b**). The error bars represent the standard deviations measured by three independent measurements

Optimization of method

The following parameters were optimized: (a) Sample pH value; (b) Concentration of H_2O_2; (c) Temperature; (4) Incubation time. Respective text and Figures on optimizations are given in the Electronic Supporting Material (Fig. S3). In short, the following experimental conditions were found to give best results: (a) Best sample pH value: 7.4; (b) Best concentration of H_2O_2: 2 mM; (c) Best temperature: 37 °C; (d) Best incubation time: 60 min.

Electrochemical detection of thrombin

Under the optimal conditions, the electrochemical aptasensors were incubated in different concentrations of thrombin. As shown in Fig. 3a and b, the DPV peak current increases at around 0.28 V with increasing the concentration of thrombin (from 10 fM to 1 μM). Homogeneous aptasensor exhibits a good linear relationship between the peak current and the logarithm of thrombin concentration (logC) ranging from 10 fM to 100 nM. The equation of linear regression is I = 0.3750 logC +5.322 (R^2 = 0.9944) with the limit of detection (LOD) is 0.8 fM according to the 3σ rule (where σ is the standard deviation of ten times measurement for blank). This aptasensor is superior in sensitivity and linear range better than some other reported assays with complicated signal amplification approaches (Table 1).

The specificity of the aptasensor was investigated by detection of thrombin, Lyz, BSA, and the mixture of them (Lyz: 10 μM; BSA: 100 μM; Thb: 1 nM). As shown in Fig. 4, it can be observed that this aptasensor shows low electrochemical signals for the Lyz and BSA, which are similar to the signal for blank. However, it produces significant electrochemical signals upon the addition of thrombin. These results clearly demonstrate that the electrochemical aptasensor shows excellent specificity for the target protein, which attributes to the highly specific recognition of aptamer to its target.

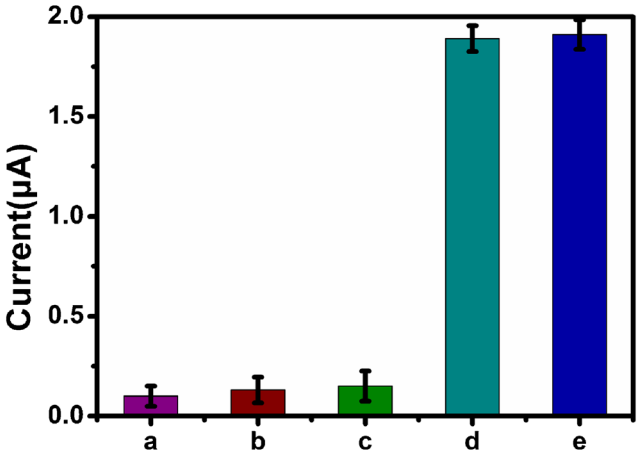

Fig. 4 Current intensity of electrochemical aptasensors to blank (a), 10 μM Lyz (b), 100 μM BSA (c), 1 nM thrombin (d) and mixture of them (e). The error bars represent the standard deviations measured by three independent measurements

The reproducibility and stability of the fabricated aptasensors were also evaluated. Under the same experimental condition, the relative standard deviation (RSD) of 4.15% was obtained for the detection of 1 μM thrombin by using four parallel aptasensors (four different aptasensors with the same fabrication procedure). Similarly, the same aptasensor was used to detect 1 μM thrombin for four times. The RSD of 4.32% can be obtained, demonstrating that the reproducibility of the aptasensor is acceptable. The stability of the aptasensor was firstly evaluated through scanning 20 times continuously with DPV measurements when the concentration of thrombin was 1 μM. As shown in Fig. S4, there is no obvious change of the DPV current. Secondly, the aptasensor was evaluated through long-term storage at 4 °C and then reacted with the supernatant produced by 1 μM thrombin as shown in Fig. S5. It can be obtained that the recorded change in the response is less than 5.7% of the initial value. All the results indicate that the aptasensor possesses acceptable stability.

Table 1 Comparison of different methods for thrombin detection

Amplification strategy	Electrochemical measurement	Linear range	Detection limit	Ref.
AuNPs and catalytic reactions of HRP	DPV [a]	0.1 pM-60 pM	30 fM	[24]
Co-catalysis of hemin/G-quadruplex, Pt NPs and MWCNT-MnO_2	DPV	1 pM-30 nM	0.04 pM	[25]
Electrocatalysis of hemin/ G-quadruplex and nanocomposite	DPV	0.05 pM-60.0 nM	15 fM	[26]
Binding-induced DNA walker-assisted	ACV [b]	10 pM-100 nM	2.5 pM	[27]
Hybridization chain reaction	DPV	10 fM - 1.0 nM.	3.5 fM	[28]
RCA triggering the combination of poly adenine with AuNPs	DPV	0.1 pM-10 nM	35 fM	[29]
TSDR-mediated proximity binding	SWV [c]	0.05 nM–100 nM	23.6 pM	[30]
Porous carbon materials and homogeneous detection	DPV	10 fM-100 nM	0.8 fM	This work

[a] Differential pulse voltammetry

[b] Alternating current voltammetry

[c] Square wave voltammetry

Real sample analysis

In order to evaluate the analytical reliability and real applicability of the fabricated aptasensor, spike and recovery experiments were performed. Human serum samples were obtained from healthy volunteers and diluted 100 times [31]. The treatment procedure and detection results are shown in in the Electronic Supporting Material (Table S2). The aptasensor did not detect thrombin in the serum sample. The reason is that serum of healthy subjects does not contain detectable thrombin [32]. When serum samples were spiked with 10 nM and 100 nM thrombin, the recoveries were between 98.14% and 99.4% and the RSDs were 3.89% and 4.01%, which were obtained from three independent experiments. Therefore, the results indicated that the fabricated aptasensors performed good applicability and reliability.

Discussion

Results show that we have proposed a new strategy to detect thrombin. However, there are two major limitations of this method: (a) Porous carbon was prepared under 1000 °C, and it does not comply with environmentally friendly chemistry. (b) During the experiment, the sample matrix was not removed, which will cause inaccurate results.

Conclusion

A sensitive homogeneous electrochemical aptasensor has been proposed based on zeolitic-imidazole framework (ZIF-8) derived porous carbon for thrombin detection. The porous carbon nanostructure and high specific surface area of the porous carbon nanomaterial Z-1000 improves electron transfer and aptameras adsorption efficiency. The results showed that the aptasensor has high sensitivity, good selectivity and high speed towards the thrombin detection. The aptasensor was also successfully applied in real samples and received good recovery. Therefore, the method provides a new strategy to fabricate other homogeneous electrochemical aptasensor using porous carbon.

Acknowledgements The research is supported from by the Natural Science Foundation of Shandong (ZR2016BM21), the Taishan Scholar Program of Shandong Province (No.ts201511027) and the National Natural Science Foundation of China (21645007).

Compliance with ethical standards

Conflict of interest The authors declare that they have no conflict of interest.

References

1. Hughes Z, Walsh T (2017) Structural disruption of an adenosine-binding DNA aptamer on graphene: implications for Aptasensor design. ACS Sensors 2:1602–1611. https://doi.org/10.1021/acssensors.7b00435
2. Xing H, Zhang C, Ruan G, Zhang J, Hwang K, Liu Y (2016) Multimodal detection of a small molecule target using stimuli-responsive liposome triggered by aptamer–enzyme conjugate. Anal Chem 88:1506–1510. https://doi.org/10.1021/acs.analchem.5b04031
3. Oishi M, Nakao S, Kato D (2014) Enzyme-free fluorescent-amplified aptasensors based on target-responsive DNA strand displacement via toehold-mediated click chemical ligation. Chem Commun 50:991–993. https://doi.org/10.1039/C3CC48064J
4. Cao X, Xia J, Liu H, Zhang F, Wang Z, Lu L (2017) A new dual-signalling electrochemical aptasensor with theintegration of "signal on/off" and "labeling/label-free" strategies. Sensors Actuators B Chem 239:166–171. https://doi.org/10.1016/j.snb.2016.08.009
5. Zhang Y, Xia J, Zhang F, Wang Z, Liu Q (2018a) A dual-channel homogeneous aptasensor combining colorimetric with electrochemical strategy for thrombin. Biosens Bioelectron 120:15–21. https://doi.org/10.1016/j.bios.2018.08.031
6. Wang S, Dong Y, Liang X (2018) Development of a SPR aptasensor containing oriented aptamer for direct capture and detection of tetracycline in multiple honey samples. Biosens Bioelectron 109:1–7. https://doi.org/10.1016/j.bios.2018.02.051
7. Tan Y, Wei X, Zhao M, Qiu B, Guo L, Lin Z, Yang H (2015) Ultraselective homogeneous electrochemical biosensor for DNA species related to Oral Cancer based on nicking endonuclease assisted target recycling amplification. Anal Chem 87:9204–9208. https://doi.org/10.1021/acs.analchem.5b01470
8. Zhang Y, Xia J, Zhang F, Wang Z, Liu Q (2018b) Ultrasensitive label-free homogeneous electrochemical aptasensorbased on sandwich structure for thrombin detection. Sensors Actuators B Chem 267:412–418. https://doi.org/10.1016/j.snb.2018.04.053
9. Cao X, Xu J, Xia J, Zhang F, Wang Z (2017) A new dual-signalling electrochemical aptasensor with the integration of "signal on/off" and "labeling/label-free" strategies. 2018. Sensors Actuators B Chem 255:2136–2142. https://doi.org/10.1016/j.snb.2016.08.009
10. Hu M, Reboul J, Furukawa S, Torad NL, Ji Q, Srinivasu P, Ariga K, Kitagawa S, Yamauchi Y (2012) Direct carbonization of Al-based porous coordination polymer for synthesis of Nanoporous carbon. J Am Chem Soc 134:2864–2867. https://doi.org/10.1021/ja208940u
11. Jiang HL, Xu Q (2011) Porous metal-organic frameworks as platforms for functional applications. Chem Commun 47:3351–3370. https://doi.org/10.1039/c0cc05419d
12. Song LF, Zhang J, Sun LX, Xu F (2012) Mesoporous metal-organic frameworks: design and applications. Energy Environ Sci 5:7508–7520. https://doi.org/10.1039/C2EE03517K
13. Fernandes DM, Barbosa ADS, Pires J, Balula SS, Cunha-Silva L, Freire C (2013) Novel composite material Polyoxovanadate@MIL-101(Cr): a highly efficient electrocatalyst for ascorbic acid oxidation. ACS Appl Mater Interfaces 5:13382–13390. https://doi.org/10.1021/am4042564
14. Yaghi OM, O'Keeffe M, Ockwig NW, Chae HK, Eddaoudi M, Kim J (2003) Reticular synthesis and the design of new materials. Nature. 423:705–714. https://doi.org/10.1038/nature01650
15. Allendorf M, Hulvey Z, Gennett T, Ahmed A, Autrey T, Camp J, Cho E, Furukawa H, Haranczyk M, Head-Gordon M, Jeong S, Karkamkar A, Liu D, Long J, Meihaus K, Nayyar I, Nazarov R, Siegel D, Stavila V, Urban J, Veccham S, Wood B (2018) An assessment of strategies for the development of solid-state adsorbents for vehicular hydrogen storage. Energy Environ Sci 11:2784–2812. https://doi.org/10.1039/c8ee01085d

16. Zhu R, Ding J, Xu Y, Yang J, Xu Q, Pang H (2018) π-Conjugated molecule boosts metal–organic frameworks as efficient oxygen evolution reaction catalysts. Small 14:1803576. https://doi.org/10.1002/smll.201803576
17. Zhu X, Zheng H, Wei X, Lin Z, Guo L, Qiu B, Chen G (2013) Metal-organic framework (MOF): a novel sensing platform for biomolecules. Chem Commun 49:1276–1278. https://doi.org/10.1039/c2cc36661d
18. Tan H, Tang G, Wang Z, Li Q, Gao J, Wu S (2016) Magnetic porous carbon nanocomposites derived from metal-organic frameworks as a sensing platform for DNA fluorescent detection. Anal. Chim. Acta 940:136–142. https://doi.org/10.1016/j.aca.2016.08.024
19. Kaneti YV, Tang J, Salunkhe RR, Jiang X, Yu A, Wu K, Yamauchi Y (2017) Nanoarchitectured Design of Porous Materials and Nanocomposites from metal-organic frameworks. Adv Mater 29:1604898. https://doi.org/10.1002/adma.201604898
20. Huang X, Lin Y, Zhang J, Chen X (2006) Ligand-directed strategy for zeolite-type metal–organic frameworks: zinc(II) imidazolates with unusual zeolitic topologies. Angew Chem Int Ed 45:1557–1559. https://doi.org/10.1002/anie.200503778
21. Yuan Y, Xia J, Zhang F, Wang Z, Liu Q (2018) Nafion/polyaniline/Zeolitic Imidazolate Framework-8 nanocomposite sensor for the electrochemical determination of dopamine. J Electroanal Chem 824:147–152. https://doi.org/10.1016/j.jelechem.2018.07.048
22. Xu J, Xia J, Zhang F, Wang Z (2017) An electrochemical sensor based on metal-organic framework-derived porous carbon with high degree of graphitization for electroanalysis of various substances. Electrochim. Acta 251:71–80. https://doi.org/10.1016/j.electacta.2017.08.114
23. Pan Y, Liu Y, Zeng G, Zhao L, Lai Z (2011) Rapid synthesis of zeolitic imidazolate framework-8 (ZIF-8) nanocrystals in an aqueous system. Chem Commun 47:2071–2073. https://doi.org/10.1039/c0cc05002d
24. Zhao J, Zhang Y, Li H, Wen Y, Fan X, Lin F, Tan L, Yao S (2011) Ultrasensitive electrochemical aptasensor for thrombin based on the amplification of aptamer-AuNPs-HRP conjugates. Biosens Bioelectron 26:2297–2303. https://doi.org/10.1016/j.bios.2010.09.056
25. Xu W, Xue S, Yi H, Jing P, Chai Y, Yuan R (2015) A sensitive electrochemical aptasensor based on the co-catalysis of hemin/G-quadruplex, platinum nanoparticles and flower-like MnO2 nanosphere functionalized multi-walled carbon nanotubes. Chem Commun 51:1472–1474. https://doi.org/10.1039/c4cc08860c
26. Wu Y, Zou L, Lei S, Yu Q, Ye B (2017) Highly sensitive electrochemical thrombin aptasensor based on peptide-enhanced electrocatalysis of hemin/G-quadruplex and nanocomposite as nanocarrier. Biosens Bioelectron 97:317–324. https://doi.org/10.1016/j.bios.2017.06.023
27. Ji Y, Zhang L, Zhu L, Lei J, Wu J, Ju H (2017) Binding-induced DNA walker for signal amplification in highly selective electrochemical detection of protein. Biosens Bioelectron 96:201–205. https://doi.org/10.1016/j.bios.2017.05.008
28. Wang C, Qian Y, Zhang Y, Meng S, Wang S, Li Y, Gao F (2017) A novel label-free and signal-on electrochemical aptasensor based on the autonomous assembly of hemin/G-quadruplex and direct electron transfer of hemin. Sensors Actuators B Chem 238:434–440. https://doi.org/10.1016/j.snb.2016.07.086
29. Fan T, Du Y, Yao Y, Wu J, Meng S, Luo J, Zhang X, Yang D, Wang C, Qian Y, Gao F (2018) Rolling circle amplification triggered poly adenine-gold nanoparticles production for label-free electrochemical detection of thrombin. Sensors Actuators B 266:9–18. https://doi.org/10.1016/j.snb.2018.03.112
30. Yang J, Wu Y, Gan C, Yuan R, Xiang Y (2018) Target-programmed and autonomous proximity binding aptasensor for amplified electronic detection of thrombin. Biosens Bioelectron 117:743–747. https://doi.org/10.1016/j.bios.2018.06.069
31. Zhao Q, Li XF, Le XC (2011) Aptamer capturing of enzymes on magnetic beads to enhance assay specificity and sensitivity. Anal Chem 83:9234–9236. https://doi.org/10.1021/ac203063z
32. Shuman MA, Majerus PW (1976) The measurement of thrombin in clotting blood by radioimmunoassay. J Clin Invest 58:1249–1258. https://doi.org/10.1172/JCI108579